

# Modeling the Growth and Molecular Structure of Electrically Conducting Polymers: Application to Polypyrrole

Jean-Christophe Lacroix,\* Rui-Jorge Valente, François Maurel, and Pierre-Camille Lacaze

**Abstract:** The growth of polypyrrole generated by electrochemical oxidation of the monomer was studied by two modeling approaches. The first is based on transition state calculations of successive coupling reactions to yield the polymer. The second evaluates the activation energy of coupling reactions by means of the frontier orbital model. The two methods predict a growth trend for polypyrrole in agreement with the structure inferred from spectroscopic investigations and provide a description of the electronic modifications induced by

the growth of the highly conjugated structure. The first approach overestimates electrostatic interactions between the two reacting species, whereas the second neglects these interactions but exaggerates the importance of orbital interactions. Combining these two approaches allows separation of the elec-

tronic effects and leads to general rules for their evolution and their impact on the growth of polypyrrole. A theoretical framework capable of rationalizing solvent and counterion effects in electropolymerization is proposed. The first approach suggests a mechanism for defect formation which excludes reactions between a pyrrole radical cation and a nonterminal monomer unit of an oligomer chain. Oxidation of the successive oligomers at high doping levels is shown to be a key factor for the growth of long, regular polymer structures.

**Keywords:** ab initio calculations • density functional calculations • polymerizations • polypyrrole • semi-empirical modeling

## Introduction

Considerable effort has been devoted to preparing electrically conducting organic polymers which consist of chains with alternating single and double bonds. They have been proposed for applications in batteries,<sup>[1]</sup> biosensors,<sup>[2]</sup> protective coatings for metals,<sup>[3]</sup> conductive photoresists,<sup>[4]</sup> optical switches,<sup>[5]</sup> and electrochromic<sup>[6]</sup> and electroluminescent<sup>[7]</sup> devices. However, they are difficult to characterize because of their very low solubility in common solvents. For this reason, their molecular structures have been proposed on the basis of various surface-science spectroscopic techniques (XPS, IR, Raman).

Electropolymerization is one of the most valuable techniques for obtaining conductive polymers. The first step of the process is a one-electron electrooxidation of the monomer, which forms a very reactive radical cation in the vicinity of the electrode. The polymer is generated by a succession of coupling reactions involving this radical cation. While many studies have been devoted to determining the properties of these materials, only a few attempts have been made to

elucidate the mechanism of electropolymerization. Several electrochemical studies on the dimerization step<sup>[8]</sup> led to the conclusion that it involves coupling of two radical cations. The subsequent coupling reactions which generate the polymer are little known and are generally considered to be similar to the dimerization step. Two pathways can be considered for the synthesis of long polymer chains: monomer–oligomer and oligomer–oligomer reactions. It is generally accepted that the former is predominant, and several experimental observations, such as the structural differences between polypyrrole and poly(bipyrrole) and the recent work of Barbarella et al.<sup>[9]</sup> on the oligomerization of 3-(alkylsulfanyl)thiophenes, support this idea. However, it was also demonstrated that terpyrrole, bipyrrole, and pyrrole radical cations have similar lifetimes in acetonitrile<sup>[10]</sup> (rate constants for dimerization:  $5 \times 10^8$ ,  $1.2 \times 10^9$ , and ca.  $10^9 \text{ M}^{-1} \text{ s}^{-1}$ , respectively), whereas tetrapyrrole has a much longer lifetime. Therefore, a contribution of oligomer–oligomer reactions to the growth of polypyrrole cannot be excluded, and they presumably compete with monomer–oligomer reactions. Here we assume that long polymer chains are obtained by successive monomer–oligomer coupling reactions; growth by oligomer–oligomer reactions will be addressed elsewhere.

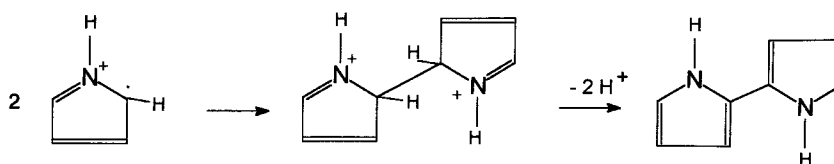
Mechanism schemes, based on the spectroscopically determined structure, have been formulated with the mesomeric forms of the radical cation generated by oxidation of the monomer. However, such schemes give no indication of the driving forces for bond formation and can neither predict the

[\*] J.-C. Lacroix, R.-J. Valente, F. Maurel, P.-C. Lacaze  
Institut de Topologie et de Dynamique des Systèmes de  
l'Université Paris 7-Denis Diderot, associé au CNRS (URA 34)  
1 rue Guy de la Brosse, 75005 Paris (France)  
Fax: (+33) 144276814  
E-mail: lacroix@paris7.jussieu.fr

most reactive sites nor consider the electronic modifications that are induced by the growth of a highly conjugated system.

Molecular modeling methods make it possible to propose new mechanistic approaches, which, in association with spectroscopic techniques, are useful tools in elucidating the polymer structure and in understanding the factors which affect electropolymerization. Few quantum chemical studies have focused on the polymerization process.<sup>[11–16]</sup> Recently, the polymerization of aniline derivatives was examined<sup>[16]</sup> by density functional calculations and discussed in terms of the softness/hardness concept; however, the study was restricted to the dimerization reaction.

Here the mechanism of electropolymerization is described by means of molecular modeling. Quantum chemical calculations were used to describe the successive coupling reactions between the monomer and oligomers of increasing length. The first objective was to determine which method is appropriate, in terms of calculation time and accuracy, for the treatment of polymer growth. The methods were evaluated by running calculations on the synthesis of polypyrrole, one of the best studied conducting polymers and one whose structure is well known. Given that there are several potential sites for attack of a pyrrole radical cation on oligomers of increasing length, correct prediction of the regioselectivity of each coupling reaction is crucial. Initially we restricted our study to the formation of the protonated dicationic intermediate (Scheme 1), because this step determines the regioselectivity of the process.<sup>[17]</sup> There is good theoretical and



Scheme 1.

experimental evidence that dimerization precedes deprotonation,<sup>[8, 18]</sup> and this mechanism is thermodynamically and kinetically favored. The second objective was understanding the factors that cause the dimerization reaction to follow a mechanism involving the coupling of two radical cations instead of one in which a radical cation attacks a neutral monomer. Can we predict the experimental conditions that will favor one of these two mechanisms? A third objective is to understand chain – monomer reactions. These are generally regarded as being analogous to the dimerization reaction, in spite of the fact that the electronic structure of the successive oligomers must evolve as the chain length grows. Few experimental data are available on these reactions, but understanding them is crucial for determining the effects that favor the synthesis of long, regular chains without structural defects.

## Methods of Calculation

The relative activation energies and hence the selectivities of the coupling reactions at various reactive sites (from the Arrhenius equation,  $T = 298$  K), were evaluated by two approaches.

The first approach was the calculation of transition states. The reaction-coordinate procedure was used to explore the region of the potential energy surface that contains a transition state (TS) by means of energy calculations on the supermolecule formed from the two reactive species. Owing to the size of the molecules to be handled (up to the hexamer), a semiempirical method is required for TS searches. The AM1 method<sup>[19]</sup> was preferred to PM3<sup>[20]</sup> since the latter predicts unrealistic partial charges on nitrogen atoms, whereas AM1 provides reliable results for aromatic compounds and gives good predictions of the dissociation energies of radical cations.<sup>[21]</sup> All geometries were optimized without symmetry constraints. Application of the semiempirical method AM1(UHF) to the reaction between two pyrrole radical cations gave potential energy/reaction coordinate curves of the same general form for the different coupling sites. The energy barrier corresponds to a well defined transition state since the diagonalized force-constant matrix contains only one negative eigenvalue, and animation of the vibrations indicates that the transition states connect the correct reactants and products, that is, bond formation and bond breaking correspond to the forward and backward reactions.<sup>[22]</sup> This approach required relative activation energies, which were initially calculated at the semiempirical AM1 level, since semiempirical energies are generally adequate for determination of regioselectivity.<sup>[23]</sup> The correlation energy was taken into account by combining of semiempirical AM1 optimized geometries with MP2<sup>[24]</sup> and DFT single-point calculations (MP2/6-31G\*//AM1 and B3LYP/6-31G\*//AM1). The hybrid Becke3LYP method was used for the DFT calculations and was preferred to MP2/6-31G\*//AM1 for studying the polymerization steps since it gives correlation effects at the cost of a simple ab initio calculation. This is the Becke three-parameter functional<sup>[25]</sup> with nonlocal correction provided by the LYP expression.<sup>[26]</sup> According to this procedure, absolute activation energies are not calculated accurately, and it is assumed that errors in the activation energies of two similar reactions are similar, so that the calculated differences are significant. This must be kept in mind when analyzing the results. Accurate computation of absolute energies remains a

**Abstract in French:** *La croissance électrochimique du polypyrrole a été modélisée par deux approches théoriques différentes. La première repose sur le calcul des états de transition des réactions de couplage conduisant à l'obtention du polymère. La deuxième évalue l'énergie d'activation des ces réactions dans le cadre du modèle des orbitales frontières. Les deux méthodes prédisent une structure pour le polymère en accord avec celle proposée à partir des données expérimentales et décrivent les modifications électroniques induites par la croissance de la structure conjuguée. La première approche surestime les interactions électrostatiques entre les espèces qui se couplent alors que la seconde approche néglige complètement ces interactions et exagère ainsi l'importance des interactions orbitales. La combinaison de ces deux approches permet donc de séparer les effets électroniques et conduit à des règles sur leurs évolutions et leurs impacts respectifs pendant la croissance du polypyrrole. Un cadre théorique, susceptible de rationaliser les effets de solvant et de contre ion dans les processus d'électropolymérisation est ainsi établi. Par ailleurs, la première approche suggère un mécanisme de formation des défauts dans le matériau qui exclue les réaction entre un radical cation pyrrole et un oligomère via un motif central de l'oligomère. De plus, les deux approches indiquent que l'oxydation des oligomères à des forts taux de dopage est un paramètre essentiel de l'obtention de chaînes longues et sans défauts structuraux.*

major challenge, requires excessive calculation times, and is beyond the scope of this work.

The second approach evaluates the activation energy of the successive reactions that lead to the polymer by means of the frontier orbital model. In this strategy, calculation of the electronic structure of the reacting species involved in the growth of the polymer is the only requirement and no information on the transition states of the reactions is obtained. The semiempirical AM1 method was used with full geometry optimization. Calculations were performed with UHF and RHF methods. Both gave essentially the same results for the major coupling of each step and for the overall trend as the oligomer length increases. Since the frontier orbital model is derived from a Hückel approach to the chemical bond, the restricted Hartree–Fock results (RHF) will be presented, although the unrestricted Hartree–Fock method (UHF) gives better results for radical structures.<sup>[27]</sup>

All semiempirical calculations were performed with the MOPAC 7 program. Gaussian 94 was used for ab initio and DFT calculations.<sup>[28]</sup> Unless otherwise stated, all calculations refer to the gas phase. Solvent effects were modeled by the AMSOL V5.4 software<sup>[29]</sup> with the SM2 and SM4 solvation models<sup>[29]</sup> on the basis of the gas-phase optimized geometry. Furthermore, for the dimerization of pyrrole by the radical/substrate mechanism, it was found that the relaxation of the transition state geometry induced by the solvent is small. The SM2 and SM4 methods are based on atomic charges derived from the AM1 semiempirical Hamiltonians and calculate the solvation energies by using a cavity adapted to the molecular shape of the solvated molecule. For a wide range of neutral and ionic molecules they yield solvation energies with an average error of only 1–2 kcal mol<sup>-1</sup>.

## Results and Discussion

### Transition state calculations

#### 1) Dimerization step

**Radical cation/radical cation mechanism:** Table 1 lists absolute energy barriers and relative coupling rates for different coupling sites calculated by AM1, 6-31G\*//AM1, MP2/6-

Table 1. Activation energies relative to the reactants (in kcal mol<sup>-1</sup>) and relative rates of the different coupling reactions (ratios between the calculated coupling rates for different coupling sites and the highest calculated coupling rate) calculated by means of different modeling methods for pyrrole dimerization by the radical cation/radical cation mechanism.

		AM1	631G*//AM1	MP2/6-31G*//AM1	B3LYP/6-31G*//AM1
$\alpha-\alpha$	energy barriers [kcal mol <sup>-1</sup> ]	74.8	94.6	58.1	60.6
	relative rates	1	1	1	1
$\alpha-\beta$	energy barriers [kcal mol <sup>-1</sup> ]	75.2	102.2	61.6	65.7
	relative rates	0.5	10 <sup>-6</sup>	3 × 10 <sup>-3</sup>	2 × 10 <sup>-4</sup>
$\beta-\beta$	energy barriers [kcal mol <sup>-1</sup> ]	75.4	109.5	65.7	70.8
	relative rates	0.3	10 <sup>-11</sup>	10 <sup>-6</sup>	10 <sup>-8</sup>

31G\*//AM1, and B3LYP/6-31G\*//AM1 for the reaction between two pyrrole radical cations. Ab initio and DFT results clearly indicate that the major coupling mode involves the C2 carbon atoms of the two radical cations. This is in agreement with experimental results. Electron correlation is very important and lowers the barriers considerably (on going from 6-31G\*//AM1 to MP2/6-31G\*//AM1). The MP2/6-31G\*//AM1 and B3LYP/6-31G\*//AM1 results give similar absolute energy barriers. Therefore, the latter method was used for the following steps of the growth process. As expected, the use of semiempirical methods with the UHF formalism yielded inaccurate results.<sup>[23c]</sup> Furthermore, semiempirical calculations underestimate energy differences between the transition states and therefore indicate lower regioselectivity than the ab initio calculations.

This approach allows a relatively precise description of the geometry of the transition states of these coupling reactions. This is in general experimentally inaccessible. The evolutions of the AM1-calculated geometry and of the HOMO for the C2–C2' coupling of the supermolecule formed by the two reactive species are shown in Figures 1 and 2. The major interaction between the two radical cations involves the  $\pi$  orbitals. When two pyrrole radical cations approach one another, the carbon 2p<sub>z</sub> orbitals overlap significantly, and the two molecules come together with their planes roughly parallel. Consequently, these orbitals are brought approx-



Figure 1. Evolution of the geometry for the  $\alpha-\alpha$  coupling of two pyrrole radical cations; a)  $d_{c-c} = 2.5$  Å; b) transition state; c) dihydropyrrole dication.

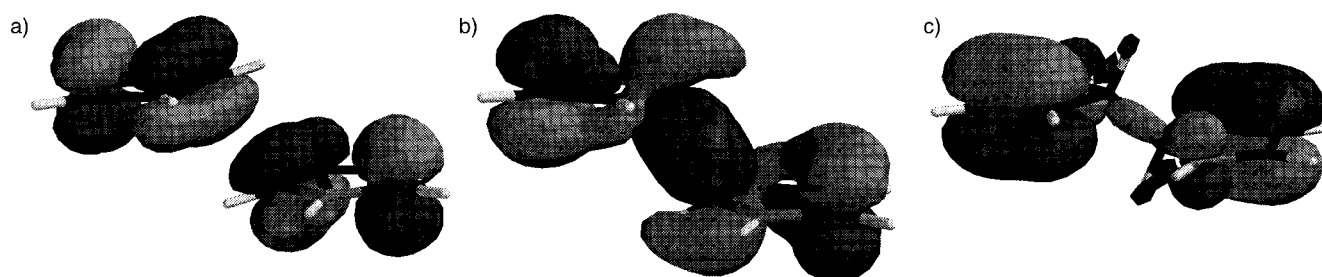
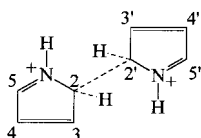


Figure 2. Evolution of the supermolecule HOMO for the  $\alpha-\alpha$  coupling of two pyrrole radical cations. a)  $d_{c-c} = 2.5$  Å; b) transition state; c) dihydropyrrole dication.

Table 2. Main AM1-calculated geometric parameters for the species involved in the  $\alpha$ - $\alpha$  dimerization of pyrrole by the radical cation/radical cation mechanism.

	N–C5 [Å]	C4–C5 [Å]	C3–C4 [Å]	C2–C3 [Å]	N–C2 [Å]	C2–H [Å]	C2–C2' [Å]
pyrrole radical cation	1.384	1.467	1.382	1.467	1.384	1.101	-
transition state	1.350	1.480	1.383	1.472	1.434	1.103	2.199
dimer dication	1.335	1.474	1.364	1.530	1.488	1.137	1.543
bipyrrole	1.389	1.406	1.429	1.415	1.400	-	1.435

imately into a  $\sigma$ -type overlap. This induces ring deformation, and the hydrogen atoms linked to the coupling carbon centers move out of the molecular planes. The intermediate dimeric dication has tetrahedral carbon centers which are  $sp^3$ -hybridized and prevent conjugation between the rings. This sequence is confirmed by analyzing the variations in the interatomic distance and  $\pi$ -electron delocalization during the formation of bipyrrole. The main geometric characteristics of the species involved are listed in Table 2.

The C2–C2' distance in the transition state is 2.2 Å, which is a normal distance for carbon–carbon bond formation in transition states.<sup>[30]</sup> The corresponding distance in the stable protonated dimeric dication is 1.543 Å, which is indicative of a C–C single bond between the  $sp^3$  carbon atoms of the two reactants. The aromatic character of the rings, which is already partially lost in the radical cation, disappears in the transition state and in the protonated dimeric dication because these  $sp^3$  carbon centers prevent conjugation. The dramatic decrease in the C3–C4 and N–C5 distances indicates a more pronounced double-bond character. The N–C2 distance increases and becomes a single bond length during coupling. The loss of two protons regenerates the aromatic rings. Table 2 shows that the pronounced single- and double-bond character of the dimeric dication are much less evident in bipyrrole.

**Radical cation/substrate mechanism:** The dimerization mechanism is considered to be a radical cation/radical cation process but earlier studies suggested a radical cation/substrate mechanism.<sup>[31]</sup> Under the conditions of electrochemical synthesis, the local concentrations of radical cations and unoxidized monomer are roughly equal, and this implies that the frequencies of encounters between two radical cations and between a radical cation and a molecule are similar. The two mechanisms could therefore compete, and the nature of the solvent and other experimental parameters may favor one of the mechanisms. We therefore studied the radical cation/substrate mechanism to understand the factors involved.

Two pyrrole molecules with an overall charge of +1 are brought together so as to simulate the radical cation/substrate mechanism. When the two molecules are separated, the charge is located completely on one ring, and the other is uncharged. An initial minimum on the energy profile indicates a long-range ion–dipole complex, which is more stable than the dissociated reactants. When the two molecules are brought closer together, the energy increases until the transition state is reached. The calculated geometry of the

transition state is similar to that of the radical cation/radical cation mechanism, with the two rings parallel, but the distance between the carbon atoms which couple is approximately 0.15 Å shorter. Although this calculated difference requires confirmation by higher level calculations, it is in agreement with the theoretical study of Tanaka et al.<sup>[32]</sup> The most important difference is the marked decrease in the energy barrier as compared to the radical cation/radical cation mechanism. The energy of the transition state is lower than that of the reactants but higher than that of the complex. This type of energy profile is also obtained for  $S_N2$  reactions in the gas phase.<sup>[33]</sup> Activation energies are –9.3, –8.1, and –6.2 kcal mol<sup>-1</sup> (AM1) for the C2–C2', C2–C3', and C3–C3' coupling reactions, respectively. The regioselectivity for the radical cation/substrate mechanism appears to be similar to that of the radical cation/radical cation mechanism; this means that they cannot be distinguished on this basis. However, in view of the considerable difference in the energy barriers, the radical cation/substrate mechanism is, as expected, clearly preferred in the gas phase.

**Solvent effects:** The transition state energies calculated for the radical cation/radical cation mechanism in the gas phase are high because of the electrostatic repulsion associated with the approach of two positively charged species. However, in the vicinity of the electrode solvent is present, and this plays an important role in weakening this interaction. An AM1-SM2 calculation of the energy on the basis of the optimized gas-phase geometry indicates that the solvent (here water) stabilizes the doubly charged transition state more than the reactants (two singly charged pyrrole molecules) by as much as 63 kcal mol<sup>-1</sup>. This value is largely independent of the coupling sites of the two pyrrole radical cations, and therefore solvation appears to have little impact on the regioselectivity of the process. The dimerization of two radical cations, which appeared very difficult in the gas phase, becomes feasible when solvent effects are included. They dramatically lower the activation energy of the radical cation/radical cation mechanism in aqueous solution. The same calculations on the radical cation/substrate mechanism show that the solvent stabilizes the 1+ transition state less than the reactants (one pyrrole cation and one neutral pyrrole molecule) by 17 kcal mol<sup>-1</sup>. The activation energy becomes positive and comparable to that of the radical cation/radical cation mechanism. Combining the B3YP/6-31G\*/AM1 gas-phase absolute energy barriers with the  $\Delta(\Delta G_{\text{solv}}^0)$  calculated at the

AM1-SM2 level gives an approximate energy barrier of  $-2.9 \text{ kcal mol}^{-1}$  for the radical cation/radical cation mechanism in aqueous solution and  $+1.9 \text{ kcal mol}^{-1}$  for the radical cation/substrate mechanism (C2–C2' coupling). Thus, competition between these two mechanisms can be understood only if solvent effects are taken in account. Interestingly, performing the same calculation with the AM1-SM4 model, which is parametrized to reproduce free enthalpies of solvation in hexane, leads to the prediction that in a such solvent the radical cation/substrate mechanism will remain largely dominant (radical cation/radical cation  $26.0$ , radical cation/substrate  $-9.4 \text{ kcal mol}^{-1}$ ). This last case is purely hypothetical, since in such a solvent ion pairing, which has not been modeled, occurs and weakens the electrostatic interactions. Although accurate prediction of the preferred mechanism requires higher level calculations, it is nevertheless possible to suggest that solvent effects are strong enough in water to make the radical cation/radical cation mechanism predominant, while in apolar, aprotic solvents additional reduction of the electrostatic interaction by counterion effects or ion pairing will be needed. In polar, aprotic solvents such as acetonitrile, in which it has been shown experimentally that dimerization occurs by an radical cation/radical cation mechanism, solvent effects may not be sufficiently strong to explain the experimental observations, and counterion effects could play a key role in the competition.

## 2) Chain–monomer reactions

Transition states involving an oligomer and the oxidized monomer were first calculated without solvent effects. The results are therefore perturbed by the overestimation of electrostatic interactions. Solvent effects were introduced by means of AM1-SM2 calculations of the energy on the basis of

the optimized gas-phase geometry. The calculations were performed with oligomers of increasing length. The oligomer that is kinetically favored in step  $n-1$  is chosen in step  $n$ .

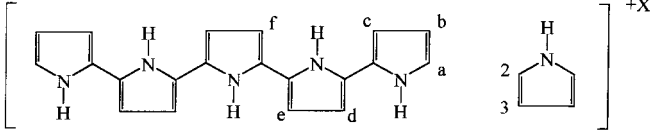
The supermolecule has a charge of  $+2$  in the trimerization and the tetramerization steps, and a charge of  $+3$  in the subsequent steps in order to maintain a charge of  $+1$  on the monomer. When the total charge in the pentamerization step is  $+2$  and the two reactants are far from each other, the charge is on the tetrapyrrole and the monomer is neutral. This recalls a well-known experimental result: it is easier to oxidize tetrapyrrole electrochemically to the dication than pyrrole to the monocation. This charge distribution does not fit the experimental observation that electropolymerization occurs only if a pyrrole radical cation is formed. Furthermore, it has been shown that polypyrrole is doped to the extent of 30–50% during its synthesis. We therefore imposed an overall charge of  $+3$  for the pentamerization and hexamerization steps and ensured that the charges were well distributed in the system when the reactants were far apart (pyrrole singly charged, oligomer doubly charged).

Calculated energy barriers and relative rates for successive coupling steps in the gas phase are listed in Table 3.

### General features of oligomerization reactions

A) *Regioselectivity and transition state structure*: The kinetically favored coupling mode involves the C<sub>a</sub> carbon atom of the oligomer and the C2 carbon atom of the monomer (AM1 and B3LYP/6-31G\*\*/AM1). This is in agreement with the structure of polypyrrole that was inferred from experimental observations. The transition state geometries of the successive predominant coupling steps appear to be very similar (Figure 3 top). The transition state for the tetramerization step consists of a terpyrrole molecule and a pyrrole molecule

Table 3. Energy barriers (in  $\text{kcal mol}^{-1}$ ) and relative rates of the different coupling reactions for pyrrole oligomerization at the B3LYP//AM1 level. Overall charge  $2+$  in the tri-, tetra-, and pentamerization steps,  $3+$  in the penta- and hexamerization steps.<sup>[a]</sup>



Coupling site	C <sub>a</sub> –C2	C <sub>a</sub> –C3	C <sub>b</sub> –C2	C <sub>c</sub> –C2	C <sub>d</sub> –C2	C <sub>e</sub> –C2	C <sub>f</sub> –C2
Trimerization							
energy barriers	<b>46.6</b>	50.1	64.8	60.8	-	-	-
relative rates	<b>1</b>	0.003	$10^{-14}$	$5.10^{-11}$	-	-	-
Tetramerization							
energy barriers	<b>35.0</b>	36.7	56.6	48.2	52.0	-	-
relative rates	<b>1</b>	0.06	$10^{-16}$	$10^{-10}$	$4 \times 10^{-13}$	-	-
Pentamerization (overall 2+ charge)							
energy barriers	<b>25.9</b>	28.2	46.1	-	42.0	38.0	-
relative rates	<b>1</b>	0.02	$10^{-14}$	-	$10^{-12}$	$10^{-9}$	-
Pentamerization (overall 3+ charge)							
energy barriers	<b>83.4</b>	86.7	95.6	99.6	105.4	116.2	-
relative rates	<b>1</b>	0.004	$10^{-9}$	$10^{-12}$	$10^{-16}$	$10^{-24}$	-
Hexamerization							
energy barriers <sup>[b]</sup>	<b>77.7</b>	78.6	83.4	88.6	96.6	97.8	97.1
relative rates <sup>[b]</sup>	<b>1</b>	0.2	$7 \times 10^{-5}$	$10^{-8}$	$2 \times 10^{-14}$	$2 \times 10^{-15}$	$6.10^{-15}$
	<b>1</b>	0.02	$10^{-10}$	-	-	-	$10^{-22}$

[a] The major product of the step is indicated in bold type. [b] AM1//AM1 results, B3LYP//AM1 results

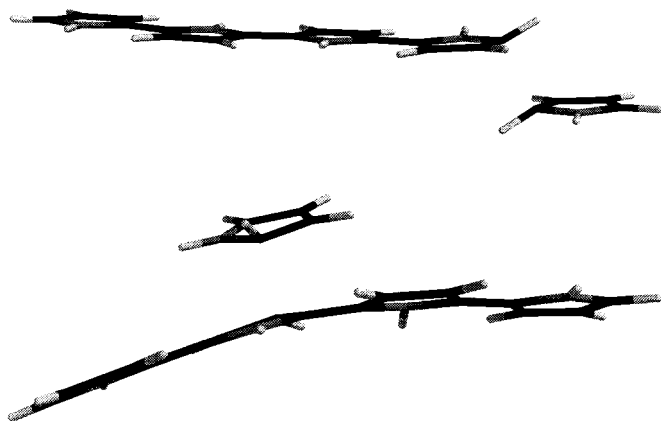


Figure 3. Geometry of the transition state during the pentamerization step. Top: For  $C_\alpha$ -C2 coupling; bottom: For  $C_\beta$ -C2 coupling.

in two parallel planes. The two hydrogen atoms linked to the carbon atoms that couple lie out of the planes of the molecules, and further evolution towards the tetramer dication increases the dihedral angles between the ring planes and the  $C_\alpha C_\beta H$  planes. Analysis of the variations of the interatomic distances and  $\pi$ -electron delocalization during the reaction leads to the same conclusion as for the dimerization step, that is, the intermediate has tetrahedral  $sp^3$  carbon centers which prevent conjugation between rings.

**B) Structural defects:** Polypyrrole contains some  $C_\alpha$ - $C_\beta$  bonds, which are regarded as defects in the polymer backbone because they prevent good conjugation.<sup>[34]</sup> The mechanism and the factors that control the number of defects in the chains are not fully understood. However, it is widely accepted that chain growth renders the  $C_\alpha$  and  $C_\beta$  atoms equivalent, and that defects are generated by coupling between  $C_\beta$  of the oligomer and C2 of the monomer. It has also been proposed that defect formation implies central chain motifs<sup>[35]</sup> or chain-chain reactions.<sup>[36]</sup>

The modeling approach developed here reveals the principal mode of defect formation in polymer chains.<sup>[37]</sup> In all the steps treated, the reaction leading to defects in polypyrrole seems to be coupling between  $C_\alpha$  of the oligomer and C3 of the monomer radical cation. The alternative route to  $C_\alpha$ - $C_\beta$  bonds—coupling between  $C_\beta$  of the oligomer and C2 of the monomer radical cation, which is the usual mode of defect formation proposed in the literature—appears to be negligible, since the most reactive site of the successive oligomers is clearly  $C_\alpha$ . Coupling between a carbon atom of the monomer and a carbon atom situated in an internal ring of the chain appears very unlikely. The probability of chain-chain reactions involving internal ring carbons would appear to be even lower. This mode of defect formation implies that once the  $C_\alpha$  carbon of an oligomer is blocked, the radical cations generated by oxidation are much more stable. This has been observed experimentally for  $\alpha$ -blocked or end-capped oligothiophenes<sup>[8b, 38]</sup>

The low reactivity of carbon atoms situated in internal units of the chains cannot be attributed to

steric effects, since the forming carbon-carbon bond is shorter for  $C_\alpha$ -C2 than for  $C_\beta$ -C2 transition states. It can be attributed to the greater loss of conjugation induced by binding a pyrrole radical cation at such positions. Indeed, the geometry in the  $C_\alpha$ -C2 transition state is predicted to differ considerably from that involving a terminal unit of the chain ( $C_\beta$ -C2). As can be seen in Figure 3 bottom, the two molecules are still in parallel planes but the tetrapyrrole molecule is severely deformed and is no longer planar (bending angle:  $15^\circ$ ). This dramatically reduces the conjugation and consequently increases the activation energy of the reaction.

**C) Solvent effects:** Solvent effects appear to be dependent on the relative coupling sites between the two reacting species. The  $\Delta(\Delta G_{\text{sol}}^0)$  values for the reaction leading to  $C_\alpha$ -C2 and  $C_\beta$ -C2 coupling are higher than those for  $C_\alpha$ -C2 and  $C_\alpha$ -C3 coupling. This is in marked contrast to the the dimerization reaction. It indicates that solvent effects will influence the regioselectivity of reactions between a pyrrole radical cation and an oligomer and lower the energy gap between the competing coupling reactions. These differences in the solvation of the various transition states can be attributed to variations in charge distribution. Charge separation is higher in the  $C_\alpha$ -C2 and  $C_\beta$ -C2 transition states than in the  $C_\alpha$ -C2 and  $C_\alpha$ -C3 transition states and leads to stronger solvation.

#### Evolution during the growth process

The evolution of properties during polymer growth is more difficult to analyze, because calculations performed on molecules with different numbers of atoms must be compared, whereas the regioselectivity of each step is based on the comparison of calculations on molecules with equal numbers of atoms. Table 4 shows the overall trend predicted for the partial charge on the pyrrole oligomers, the interatomic distance between the coupling carbon atoms in the transition states, the activation energies, and the regioselectivity at the B3LYP/6-31G\*//AM1 level (gas-phase calculations). It also shows the evolution of  $\Delta(\Delta G_{\text{sol}}^0)$  calculated by AM1-SM2 for the successive oligomerization steps. Combining the B3LYP/

Table 4. Calculated variations with chain length for the coupling of pyrrole with an oligopyrrole: Partial charge on the pyrrole moieties in TS, TS interatomic distance, B3LYP//AM1 gas phase energy barriers, gas phase regioselectivity, AM1-SM2  $\Delta(\Delta G_{\text{sol}}^0)$ , and approximate energy barriers in water.

	Dimeri- zation	Trimeri- zation	Tetra- meriza- tion	Pentamerization <sup>[a]</sup>	Hexa- meriza- tion
partial charge on pyrrole	1	0.80	0.63	(0.46) 0.84	0.73
C-C distance [Å] in TS	2.20	2.14	2.09	(2.02) 2.11	2.07
B3LYP//AM1					
gas phase energy barriers [kcal mol <sup>-1</sup> ]	60.6	46.6	35	(25.9) 83.4	68.1
B3LYP//AM1 gas phase % of defect	$2 \times 10^{-4}$	$3 \times 10^{-3}$	$6 \times 10^{-2}$	( $2 \times 10^{-2}$ ) $4 \times 10^{-3}$	$2.10^{-2}$
$\Delta(\Delta G_{\text{sol}}^0)$ AM1-SM2 (kcal mol <sup>-1</sup> )	-63.4	-47.7	-34.3	(-9.4) -69.2	-
energy barriers in water [kcal mol <sup>-1</sup> ]	-2.9	-1.1	0.6	(16.5) 14.2	-

[a] (Overall charge 2+), Overall charge 3+.

6-31G\*\*/AM1 gas-phase absolute energy barriers with the calculated  $\Delta(\Delta G_{\text{solv}}^0)$  at the AM1-SM2 level allows a crude evaluation of the activation energy barrier in aqueous solution during the growth process.

*A) Gas-phase evolutions:* Provided the same overall charge is imposed on the supermolecule, the energy barrier decreases during polypyrrole growth. The activation energy for terpyrrole formation is lower than that for dimerization. This result holds as long as the supermolecule bears the same overall charge (+2 or +3). However, when the charge increases from +2 to +3 (pentamerization step) the calculated energy barrier increases. This effect appears to be correlated with the evolution of the electrostatic repulsion between the two reacting molecules. The charge is distributed over the entire oligomer chain, and this implies that the net charge on each atom decreases when the length of the oligomer increases. This reduces the electrostatic interactions between the two molecules; consequently, the energy barrier decreases. Energy barriers increase when the charge of the system goes from +2 to +3, because the net charge on each atom and the electrostatic repulsion between the two reacting species increase. This trend does not necessarily reproduce what really happens in the growth process, since at this stage the calculations do not include solvent effects. The results are therefore distorted by the overestimation of the electrostatic interactions between the reacting species.

The observed evolution of the charge distribution between the two reacting moieties in the successive transition states indicates that pronounced electron transfer from the oligomer to the pyrrole radical cation occurs, and that this electron transfer increases with the oligomer length. At the same time, the HOMOs of the successive transition states evolve; these HOMOs appear to be a linear combination of the two SOMOs of the separated species with a small contribution of SOMO + 1 of the pyrrole radical cation (deduced by means of single-point calculation on the separated species in the transition state geometry). As the oligomer length increases, the SOMO–SOMO interaction decreases sharply, whereas the contribution of SOMO + 1 of the pyrrole radical cation to the HOMO of the transition state increases and is responsible for the increasing partial charge transfer between the two reacting species. As a consequence of these two effects, the overall orbital interaction decreases as the oligomer length increases (for a given C2–C2' distance).

The decrease in the electrostatic repulsion and of the frontier orbital interactions (for the same C2–C2' distance) as the oligomer length increases leads to a pronounced evolution of the C–C distance in the successive transition states. This distance decreases with increasing oligomer length as long as the supermolecule bears the same overall charge (+2 or +3) but increases sharply when the overall charge goes from +2 to +3. Although higher level calculations (TS geometry optimization at the ab initio level) might be needed to confirm this geometry evolution, this trend can be interpreted as follows. It is generally accepted that the more reactive a molecule is, the sooner the TS will be reached.<sup>[39]</sup> Hence, for a bond-forming reaction, the length of this bond in the transition state increases with increasing reactivity of the reactants. There-

fore, the evolution of the C–C distance in the successive transition states probably reflects the decreasing reactivity of the oligomers towards the pyrrole radical cation with increasing oligomer length. However, this evolution can generally be correlated with the value of the absolute energy barrier (according to the Hammond postulate), since it is generally observed that as the absolute energy barrier increases, the transition state is reached later in the reaction.<sup>[39]</sup> This is clearly not the case here. This contradiction suggests that the frontier orbital interaction effect has a greater influence on the geometry of the successive transition states than the electrostatic repulsion (a shorter C2–C2' distance would be needed to provide additional stabilization by stronger frontier orbital interactions in the successive transition states, but electrostatic repulsion increases with decreasing C2–C2' distances).

Table 4 also shows the evolution of the calculated regioselectivity of each step at the B3LYP/6-31G\*\*/AM1 level. As long as the supermolecule bears the same overall charge, the regioselectivity of the successive coupling steps decreases continuously. When the overall charge goes from +2 to +3, the regioselectivity increases sharply. This clearly indicates that oxidation of the oligomers at high doping levels is a key factor for the growth of long, regular polymer structures.

*B) Solvent effects:* When solvent effects are introduced into the calculations, the energy barriers become more realistic. The solvent stabilizes the transition states far more than separated radical cations. As expected  $\Delta(\Delta G_{\text{solv}}^0)$  decreases sharply as the oligomer length increases, since the overall charge is delocalized over a larger number of atoms, and partial charge transfer reduces the charge separation in the transition states. Electrostatic interactions are therefore balanced by solvation in these successive coupling reactions. Combining the B3LYP/6-31G\*\*/AM1 gas-phase absolute energy barriers with  $\Delta(\Delta G_{\text{solv}}^0)$  calculated at the AM1-SM2 level gives an approximate energy barrier for the successive C2–C2' coupling steps (Table 4). The dimerization, trimerization, and tetramerization steps have similar activation energies in aqueous solution (–2.9, –1.1 and 0.6 kcal mol<sup>–1</sup>, respectively); dimerization is the fastest process. In contrast, there is a pronounced difference between the activation energy of the tetramerization (+0.6 kcal mol<sup>–1</sup>) and the pentamerization steps (+14.2 and 16.5 kcal mol<sup>–1</sup> for an overall charge of +3 and +2, respectively). The relative rates of the dimerization, trimerization, and tetramerization steps appear to be highly dependent on the electrolytic solvent. Strong solvent screening (as in water) of the electrostatic interactions is needed to make dimerization faster than tetramerization.

**Frontier orbital model:** The main defect of the modeling approach presented above is that gas-phase results are distorted by overestimation of electrostatic interactions. Our calculations with the SM2 model, on the basis of the gas-phase optimized geometries, show that the solvent considerably lowers these interactions. A simpler and complementary approach is to analyze the successive coupling reactions with the frontier orbital model. This model postulates that the regioselectivity is controlled by interactions between the

frontier orbitals of the reacting species and completely neglects electrostatic interactions. Thus the reactions are examined from an extreme view point that exaggerates the influence of orbital interactions. This approach uses a screening effect to simulate the influence of a solvent, which considerably reduces electrostatic interactions. The suppression of all such interactions can be regarded as equivalent to the use of an imaginary solvent with maximum screening effect.

The frontier orbital model evaluates the relative activation energies by means of a simple calculation of the molecular orbitals of the separate reactants. This model does not describe the transition states but has been used successfully with several conducting polymers of known structures [12–14, 35]. It has the advantage of using few calculation resources.

Here we simply present the main results obtained for polypyrrole growth without describing the model in detail. A radical cation/radical cation mechanism was assumed. The major orbital interaction between two molecules A and B is then that between the SOMO of molecule A and the SOMO of molecule B. The ratio of two competitive coupling rates is given by Equation (1). Here  $v_{a_1 \rightarrow b}$  and  $v_{a_2 \rightarrow b}$  are the rates of

$$\frac{v_{a_1 \rightarrow b}}{v_{a_2 \rightarrow b}} = \exp\left(\frac{2(\beta_{a_1 b}^2 C_{a_1}^2 C_b^2 - \beta_{a_2 b}^2 C_{a_2}^2 C_b^2)}{kT(E_{\text{SOMO}_A} - E_{\text{SOMO}_B})}\right) \quad (1)$$

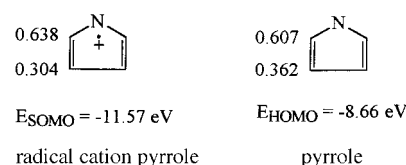
coupling of sites  $a_1$  and  $a_2$  of molecule A on site b of molecule B.  $C_a$  and  $C_b$  are the atomic orbital coefficients of atoms A and B in the molecular frontier orbitals  $\text{SOMO}_A$  and  $\text{SOMO}_B$ ,  $E_{\text{SOMO}_A}$  and  $E_{\text{SOMO}_B}$  the energies of these orbitals, and  $\beta$  the resonance integrals. Resonance integrals depend on the distance between the two coupling atoms, on the nature of the atoms, and on the semiempirical method used. The  $\beta_{\text{CC}}$  were calculated by AM1 for a  $\sigma$ -type overlap between  $2p_z$  orbitals and for interatomic distances of 1.75, 2.00, and 2.25 Å. A distance between 2 and 2.25 Å was found by transition state calculations (first approach), but since the frontier orbital model does not allow it to be determined and since the previous calculations suggested that it falls with increasing oligomer length, the coupling results are reported for several interatomic distances.

In the more general case, the  $\text{SOMO} - 1$ ,  $\text{SOMO}$ , and  $\text{SOMO} + 1$  have been used in the description of the oligomer–monomer interaction. However, the results are practically the same if only the  $\text{SOMO}$  is used, as in the case of the heptamerization step (Table 7). In the case of a dimerization reaction by a radical cation/radical cation mechanism,  $E_{\text{SOMO}_A} = E_{\text{SOMO}_B}$ , and Equation (2) is obtained.

$$\frac{v_{a_1 \rightarrow b}}{v_{a_2 \rightarrow b}} = \exp\left(\frac{2(\beta_{a_1 b} C_{a_1} C_b - \beta_{a_2 b} C_{a_2} C_b)}{kT}\right) \quad (2)$$

### 1) Dimerization step

The highest SOMO of the pyrrole radical cation is a  $\pi$  orbital, delocalized over the aromatic ring. The most important contribution to this orbital comes from the carbon atom in the position  $\alpha$  to the nitrogen atom (Scheme 2). The frontier orbital model therefore clearly indicates that the pyrrole



Scheme 2.

radical cation will react preferentially at the  $\alpha$ -carbon atom. Scheme 2 also shows the HOMO of neutral pyrrole.

**Radical cation/radical cation mechanism:** Table 5 lists the relative coupling rates for the dimerization step by a radical cation/radical cation mechanism. Frontier orbital interactions clearly indicate a preference for the  $\alpha$ - $\alpha$  dimer; the  $\alpha$ - $\beta$  and  $\beta$ - $\beta$  dimers are predicted to be generated in extremely small quantities. At shorter distances between the coupling carbon

Table 5. Predicted relative coupling rates of pyrrole dimerization for various coupling distances (ratios between the calculated coupling rates for different sites and the highest calculated rate).

Distance [Å]	$\alpha$ - $\alpha$	$\alpha$ - $\beta$	$\beta$ - $\beta$
1.75	1	$8.10^{-21}$	$2.10^{-28}$
2.00	1	$2.10^{-16}$	$3.10^{-22}$
2.25	1	$5.10^{-12}$	$3.10^{-16}$

atoms, orbital interactions and apparent regioselectivity increase. It is interesting to compare these results with those obtained by the transition state approach. Both predict the  $\alpha$ - $\alpha$  dimer to be the major dimer, but with very different proportions of by-products. The transition state calculation suggests a less regioselective reaction than the frontier orbital approach, which predicts almost no byproducts. Apparently, there are two opposing electronic effects in dimerization: frontier orbital interactions favor  $\alpha$ - $\alpha$  coupling because of the high spin density on the  $\alpha$ -carbon atom of the pyrrole radical cations, whereas electrostatic interactions direct the reaction towards other coupling sites because the  $\alpha$ -carbon atoms bear most of the excess positive charge.

**Radical cation substrate mechanism:** Within the framework of the frontier orbital model, the radical cation/radical cation mechanism is greatly preferred over the radical cation/substrate mechanism. Maximum orbital interaction occurs for the first mechanism because the SOMOs of the two radical cations have the same energy (Figure 4), and the two electrons are stabilized by this interaction. The frontier orbital interaction is not so favorable for the radical cation/substrate mechanism. In this case the most important interaction is that between the SOMO of the radical cation and the HOMO of the neutral pyrrole molecule. This three-electron interaction is necessarily weaker. Furthermore, the HOMO of the neutral pyrrole molecule lies higher than the SOMO of the radical cation, and this further reduces the orbital interaction. Frontier orbital interactions favor the radical cation/radical cation mechanism, whereas electrostatic interactions suggest that the reaction should follow the radical cation/substrate mechanism.



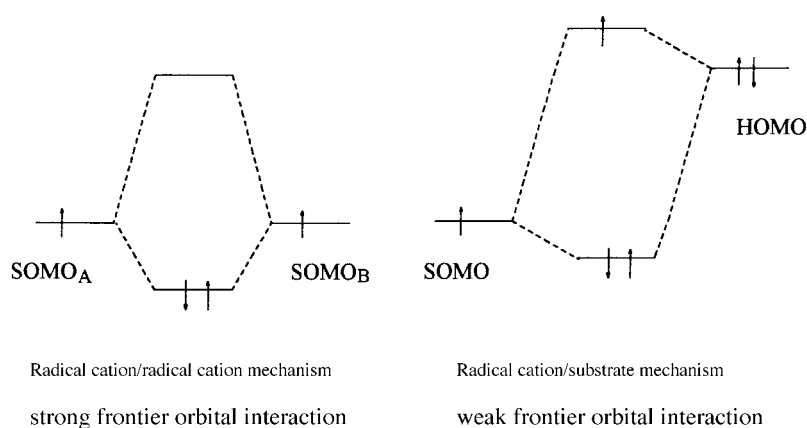


Figure 4. Frontier orbital interactions for radical cation/radical cation and radical cation/substrate mechanisms.

The frontier orbital approach simulates the influence of a solvent, which considerably reduces electrostatic interactions by a screening effect. The results obtained from the frontier orbital approach are consistent with those deduced by including solvent effects in the transition state calculations.

## 2) Polymer growth and doping levels

The regioselectivity predicted for the successive coupling steps when the successive oligomers have a charge of +1 are presented in Table 6. The major product of each step is indicated by bold type. The kinetically favored mode in all coupling steps involves the C<sub>a</sub> carbon atom of the oligomer

Table 6. Predicted relative coupling rates of pyrrole oligomerization for various coupling distances (ratios between the calculated coupling rates for different sites and the highest calculated rate).

Distance [Å]	C <sub>a</sub> -C2	C <sub>b</sub> -C2	C <sub>c</sub> -C2	C <sub>d</sub> -C2
Trimerization				
1.75	1	$2 \times 10^{-6}$	$2 \times 10^{-4}$	-
2.00	1	$3 \times 10^{-4}$	$5 \times 10^{-3}$	-
2.25	1	$2 \times 10^{-2}$	$7 \times 10^{-2}$	-
Tetramerization				
1.75	1	$10^{-3}$	$3 \times 10^{-2}$	$2 \times 10^{-2}$
2.00	1	$2 \times 10^{-2}$	$10^{-1}$	$8 \times 10^{-2}$
2.25	1	$10^{-1}$	$3 \times 10^{-1}$	$2 \times 10^{-1}$

and the C2 carbon atom of the monomer. This is in agreement with the structure of polypyrrole inferred from experimental observations and that predicted by transition state calculations. This result confirms that this approach can be used to predict the molecular structure of conducting polymers with far shorter calculation times than the transition state approach. The frontier orbital approach underlines the effect of molecular orbital overlap on the growth process. This overlap is strongly affected by binding a new monomer unit onto the chain. Three effects that appear particularly important in the first steps of polymerization can be distinguished. First, the SOMO energy of the successive oligomers increases with increasing number of monomer units. Therefore, the difference between the SOMO energy of the monomer and that of the chain increases. It is 1.97 eV for the bipyrrrole cation and

rises to 3.2 eV for the tetrapyrrole cation. As a consequence, the frontier orbital interactions between the chain and the monomer are considerably reduced. This is not surprising, since the successive oligomers are fully conjugated, so that the molecular orbitals become softer during the growth process. Second, the atomic orbital coefficients of the SOMO decrease progressively with increasing oligomer size. This is due to increasing delocalization of the molecular orbitals.<sup>[35]</sup> The SOMO atomic orbital coefficients of the two carbon atoms on the terminal monomer unit range from from 0.638–0.303 in singly charged pyrrole to 0.218–0.107 in singly charged terpyrrole. Third, as the oligomer becomes longer, the energies of SOMO, SOMO–1 and SOMO+1 become closer. The frontier orbital interactions between the growing chain and the monomer involve these orbitals, although they are three- or one-electron interactions and are therefore less strongly stabilizing than SOMO–SOMO interactions.

For successive oligomers with a charge of +1 and a constant C–C distance these evolutions of the frontier orbital interactions with increasing oligomer size induce: 1) a progressive decrease in the calculated regioselectivity of coupling reactions due to the increasing difference between the SOMO energies of the oligomer and the monomer and to the effect of the progressive decrease in the atomic orbital coefficients. (this decrease in regioselectivity is partially compensated by a progressive decrease in the C–C distance as the chain lengthens; see Table 4); and 2) a progressive increase in the activation energy of the reaction between the monomer and the chain. If it is assumed that the concentration of the monomer radical cation remains approximately constant near the electrode, then an oxidized monomer would react with another monomer radical cation rather than with a previously formed oligomer. Therefore, the growth of a long chain would be negligible compared to dimerization or the formation of small chains, and polymerization should be inhibited.

A theory consistent with the experimental observations requires factors which increase the frontier orbital interactions and hence lower the activation energy and increase the regioselectivity. Calculations suggest that the doping level of the chain has a major impact on the frontier orbital interactions and consequently on the electropolymerization process. Oxidation of the chain leads to a harder species and lowers the energy gap between its SOMO and that of the oxidized monomer. This increases the frontier orbital interaction and implies that the regioselectivity will be improved and reactions between the monomer and the chain favored. Table 7 compares the calculated regioselectivity of the

Table 7. Predicted relative coupling rates of pyrrole heptamerization for various doping levels (ratios between the calculated coupling rates for different sites and the highest calculated rate).

Distance [Å]	(17% doping level)		(50% doping level)	
	C <sub>a</sub> -C2	C <sub>b</sub> -C2	C <sub>a</sub> -C2	C <sub>b</sub> -C2
1.75	1	$10^{-1}$	1	$10^{-3}$
2.00	1	$2 \times 10^{-1}$	1	$5 \times 10^{-3}$
2.25	1	$5 \times 10^{-1}$	1	$10^{-2}$

heptamerization step of polypyrrole for a charge on the hexamer of +1 (17% doping level) with that for a charge of +3 (50% doping level). This could be a general effect applicable to most conducting polymers. Interestingly, Kobryanskii et al.<sup>[40]</sup> experimentally demonstrated for the electrosynthesis of poly(*p*-phenylene) that the degree of polymerization depends on the doping level and proposed that high doping is needed for the formation of high molecular weight polymer chains.

## Conclusions

The two approaches developed here support the molecular structure of polypyrrole that was proposed on the basis of experimental findings. They can therefore be regarded as complementary to spectroscopic methods for the structure elucidation of other polymers. The frontier orbital method requires fewer calculations, is easier to implement, and is likely to find many applications in this field.

The frontier orbital approach predicts that the radical cation/radical cation mechanism is preferred, whereas the transition state approach indicates that the two mechanisms compete and that it might be possible to find electrochemical conditions that direct the reaction towards a radical cation/substrate mechanism. While the activation energy for dimer formation is very high for the radical cation/radical cation mechanism in the gas phase (60.5 kcal mol<sup>-1</sup> at the B3LYP/6-31G\*//AM1 level), it becomes reasonable when solvent effects (SM2 model) are included. Conversely, the activation energy for the radical cation/substrate mechanism, which is negative in the gas phase, becomes positive and comparable to that of the radical cation/radical cation mechanism in solution. In water, the radical cation/radical cation reaction is predicted to be faster.

The variations of geometry and of  $\pi$ -electron delocalization during the reaction can be analysed by transition state calculations, which explore the entire reaction coordinate between the reactant species and the intermediate. This information is not accessible by experimental methods and is obtained here with relatively short calculation times. This approach also suggests a mechanism for the formation of structural defects in the chain, albeit in contradiction with the assumption that defects are created by reactions involving internal units of the chain.

An interesting feature of both approaches is that they can be used to investigate the effects of the doping level on polymer synthesis. High doping levels are associated with the formation of polymer chains with high molecular weight and few structural defects. Neither method alone is perfect, but when their shortcomings are understood (transition state calculations in the gas phase overestimate electrostatic interactions, while the frontier orbital model neglects them completely), it is possible to discern the effects of the different electronic factors on the mechanism and the outcome of chain–monomer reactions. Solvent and counterion effects in the electrochemical synthesis of conducting polymers are always important. Application of quantum chemical calculations such as those performed in this study should help to

shed some light on the polymer growth process and its dependence on monomer structure and experimental conditions.

**Acknowledgments:** We are particularly grateful to Dr J. S. Lomas (ITODYS, University of Paris 7) for revising our text and correcting the English and to Dr E. Kessab (Laboratoire de Chimie Théorique, University of Paris 6) for helpful discussions concerning transition state calculations.

Received: July 15, 1997

Revised version: April 14, 1998 [F765]

- [1] M. Angelopoulos, A. Ray, A. G. MacDiarmid, A. J. Epstein, *Synth. Met.* **1987**, *21*, 21.
- [2] a) T. A. Skotheim, H. S. Lee, P. D. Hale, H. I. Karan, Y. Okamoto, L. Samuelse, S. Tripathy, *Synth. Met.* **1991**, *41–43*, 1433; b) D. T. Hoa, T. N. S. Kumar, N. S. Puneekar, R. S. Srinivasa, R. Lal, A. Q. Contractor, *Anal. Chem.* **1992**, *64*, 2645; c) M. V. Deshpande, D. P. Amalnerkar, *Prog. Polym. Sci.* **1993**, *18*, 623.
- [3] a) C. A. Ferreira, S. Aeiyaich, M. Delamar, P. C. Lacaze, *J. Electroanal. Chem.* **1990**, *284*, 351; b) J. L. Camalet, J. C. Lacroix, S. Aeiyaich, K. Chane-Ching, P. C. Lacaze, *J. Electroanal. Chem.* **1996**, *416*, 179.
- [4] a) G. Venugopal, X. Quan, G. E. Johnson, F. M. Houlihan, E. Chin, O. Nalamasu, *Chem. Mater.* **1995**, *7*, 271; b) M. Angelopoulos, J. M. Shaw, W. S. Huang, R. D. Kaplan, *Mol. Cryst. Liq. Cryst.* **1990**, *189*, 221.
- [5] a) J. A. Osaheni, S. A. Jenekhe, H. Vanherzeele, J. S. Meth, Y. Sun, A. G. MacDiarmid, *J. Phys. Chem.* **1992**, *96*, 2830; b) C. L. Callender, L. Robitaille, M. Leclerc, *Opt. Eng. (Bellingham, Wash.)* **1993**, *32*, 2246
- [6] T. Kobayashi, H. Yoneyama, H. Tamura, *J. Electroanal. Chem.* **1984**, *161*, 419.
- [7] J. H. Burroughes, D. D. C. Bradley, A. R. Brown, R. N. Marks, K. Mackay, R. H. Friend, P. L. Burns, A. B. Homes, *Nature* **1990**, *347*, 539.
- [8] a) C. P. Andrieux, P. Audebert, P. Hapiot, J.-M. Savéant, *J. Am. Chem. Soc.* **1990**, *112*, 2439; b) P. Audebert, P. Hapiot, *Synth. Met.* **1995**, *75*, 95, and references therein; c) H. Yang, A. J. Bard, *J. Electroanal. Chem.* **1992**, *339*, 423.
- [9] G. Barbarella, M. Zambianchi, R. Di Toro, M. Colonna, D. Iarossi, F. Goldoni, A. Bongini *J. Org. Chem.* **1996**, *61*, 8285.
- [10] a) L. Guyard, P. Hapiot, P. Neta, *J. Phys. Chem. B.* **1997**, *101*, 5698; b) C. P. Andrieux, P. Hapiot, P. Audebert, L. Guyard, M. Nguyen-Dinh An, L. Groenendaal, E. W. Meijer, *Chem. Mater.* **1997**, *9*, 723.
- [11] T. P. Davis, S. C. Rogers, *Eur. Polym. J.* **1993**, *29*, 1311.
- [12] J. C. Lacroix, P. Garcia, J. P. Audié, R. Clement, O. Kahn, *New J. Chem.* **1990**, *14*, 87.
- [13] J. C. Lacroix, M. Mostefai, G. Havard, M. C. Pham, J. P. Doucet, P. C. Lacaze, *New J. Chem.* **1995**, *19*, 979.
- [14] J. C. Lacroix, G. Havard, J. J. Aaron, K. Taha-Bouamri, P. C. Lacaze, *Structural Chemistry*, **1997**, *8*, 177
- [15] J. R. Smith, P. A. Cox, S. A. Campbell, N. M. Ratcliffe, *J. Chem. Soc., Faraday Trans.* **1995**, *91*, 2331.
- [16] G. D'Aprano, E. Proynov, M. Lebeuf, M. Leclerc, D. R. Salahub, *J. Am. Chem. Soc.* **1996**, *118*, 9736
- [17] Thermodynamic control of the reaction that yields the dihydrodimer has not been investigated.
- [18] D. Larumbe, M. Moreno, I. Gallardo, J. Bertran, C. P. Andrieux, *J. Chem. Soc. Perkin Trans. 2* **1991**, *2*, 1437.
- [19] M. J. S. Dewar, E. G. Zoebisch, E. F. Hearnly, J. J. P. Stewart, *J. Am. Chem. Soc.* **1985**, *107*, 3902.
- [20] J. J. P. Stewart, *J. Comp. Chem.* **1989**, *10*, 221.
- [21] D. M. Camaioni, *J. Am. Chem. Soc.* **1990**, *112*, 9475.
- [22] MINDO/3 and PM3 were also compared with the AM1 results; the three methods converge to a similar transition state structure. Relative energy barriers for different coupling sites calculated by AM1 and MINDO/3 are similar and consistent with ab initio calculations. In contrast, PM3 calculations are in complete disagreement with the ab initio calculation. This is not surprising, since PM3 is known to predict unrealistic partial charges on nitrogen atoms.
- [23] a) G. Thoma, D. P. Curran, S. V. Geib, B. Giese, W. Damm, F. Wetterich, *J. Am. Chem. Soc.* **1993**, *115*, 8585; b) A. L. J. Beckwith,

- A. A. Zavitsas, *ibid.* **1995**, 117, 607; c) W. J. Hehre, *Practical Strategies for Electronic Structure Calculations*, Wavefunction Inc., Irvine, **1995**.
- [24] a) W. J. Hehre, L. Radom, P. von R. Schleyer, J. A. Pople, *Ab Initio Molecular Orbital Theory*, Wiley, New York, **1986**; b) C. Moller, M. S. Plesset, *Phys. Rev.*, **1934**, 46, 618.
- [25] A. D. Becke, *J. Chem. Phys.* **1993**, 98, 5648.
- [26] C. Lee, W. Yang, R. G. Parr, *Phys. Rev. B.* **1988**, 37, 786.
- [27] M. N. Paddon-Row, J. A. Pople, *J. Phys. Chem.* **1985**, 89, 2768.
- [28] M. J. Frisch, M. Head-Gordon, G. W. Trucks, J. B. Foresman, H. B. Schlegel, P. M. W. Gill, B. G. Johnson, E. S. Replogle, R. Gomperts, J. L. Andres, C. Gonzalez, D. J. Defrees, D. J. Fox, K. Raghavachari, M. A. Robb, M. W. Wong, J. S. Binkley, J. Baker, R. L. Martin, J. J. P. Stewart, J. A. Pople, GAUSSIAN 92/DFT (Revision G.4), Gaussian Inc., Pittsburgh, PA, **1993**
- [29] a) C. J. Cramer, D. G. Truhlar, *Science* **1992**, 256, 213; b) G. D. Hawkins, G. C. Lynch, D. J. Giesen, I. Rossi, J. W. Storer, D. A. Liotard, C. J. Cramer, D. G. Truhlar, QCPE program 606, version 5. 4.
- [30] K. N. Houk, Y. Li, J. D. Evamseck, *Angew. Chem.* **1992**, 104, 711; *Angew. Chem. Int. Ed. Engl.* **1992**, 31, 682
- [31] a) M. Satoh, K. Imanishi, K. Yoshino, *J. Electroanal. Chem.* **1991**, 317, 139; b) Y. Wei, C. C. Chan, J. Tian, G. W. Jang, K. F. Hsueh, *Chem. Mater.* **1991**, 3, 888.
- [32] K. Tanaka, T. Shichiri, M. Toriumi, T. Yanabe, *Synth. Met.* **1989**, 30, 271.
- [33] S. S. Shaik, H. B. Schlegel, S. Wolfe, *Theoretical Aspects of Physical Organic Chemistry: The SN2 Mechanism*, Wiley, New York, **1992**.
- [34] K. Tanaka, T. Shichiri, T. Yanabe, *Synth. Met.* **1986**, 14, 271.
- [35] R. J. Waltman, J. Bargon, *Tetrahedron* **1984**, 40, 3963.
- [36] K. Tanaka, T. Shichiri, T. Yanabe, *Synth. Met.* **1986**, 16, 207.
- [37] Coupling with formation of a C–N bond was not investigated.
- [38] P. Bäuerle, *Adv. Mater.* **1992**, 4, 102.
- [39] N. Trong Anh, F. Maurel, J. M. Lefour, *New J. Chem.* **1995**, 19, 353
- [40] V. M. Kobryanskii, S. A. Arnautov, *Synth. Met.* **1993**, 55–57, 1371.